Live-Cell Imaging and Analysis of Nuclear Body Mobility

Dmitry V Sorokin, Eugene A Arifulin, Yegor Vassetzky, Eugene V Sheval

Live-cell imaging and analysis of nuclear body mobility

Dmitry V. Sorokin[1], Eugene A. Arifulin[2,3], Yegor S. Vassetzky[3,4,5], and Eugene V. Sheval[2,3,6]

[1]Laboratory of Mathematical Methods of Image Processing, Faculty of Computational Mathematics and Cybernetics, Lomonosov Moscow State University, 119991 Moscow, Russia

[2]Belozersky Institute of Physico-Chemical Biology, Lomonosov Moscow State University, 119991 Moscow, Russia

[3]LIA 1066 LFR2O French-Russian Joint Cancer Research Laboratory, 94805 Villejuif, France

[4]Koltzov Institute of Developmental Biology of Russian Academy of Sciences, Vavilov str. 26, 119334 Moscow, Russia

[5]UMR8126, Université Paris-Sud, CNRS, Institut de cancérologie Gustave Roussy, 94805 Villejuif, France

[6]Department of Cell Biology and Histology, Faculty of Biology, Lomonosov Moscow State University, 119991 Moscow, Russia

Corresponding authors:

Yegor Vassetzky yegor.vassetzky@cnrs.fr

Eugene Sheval evsheval@gmail.com

Abstract

The cell nucleus contains different domains and nuclear bodies; their position relative to each other inside the nucleus can vary depending on the physiological state of the cell. Changes in the three-dimensional organization are associated with the mobility of individual components of the nucleus. In this paper, we present a protocol for live-cell imaging and analysis of nuclear body mobility. Unlike many similar protocols, our image analysis pipeline includes non-rigid compensation for global nucleus motion before particle tracking and trajectory analysis, leading to precise detection of intranuclear movements. The protocol described can be easily adapted to work with most cell lines and nuclear bodies.

Keywords: Nucleus, Nuclear body, Mobility, Interphase prenucleolar bodies, Particle tracking, Global non-rigid motion compensation

1 Introduction

Cell nucleus contains numerous structures referred to as nuclear bodies (NBs) [1]. The most known example of a NB is the nucleolus [2]. NBs concentrate coding and non-coding RNAs, as well as proteins which are necessary for genome functioning. The position and mobility of NBs within the nucleus play an important role in the regulation of genome functions [3]; at the same time few studies on the NB mobility exist as this is a challenging task. Here, we describe a simple and robust protocol to study the NB mobility *in vivo* and discuss technical problems and the ways to solve them using an example of experimentally induced NBs, interphase prenucleolar bodies (iPNBs). iPNBs are formed in interphase nuclei from partially disassembled nucleoli when cells return to isotonic conditions from a hypotonic shock [4]. iPNBs contain nucleolar proteins NPM1 (B23 or nucleophosmin) [4–7], NCL (C23 or nucleolin) [8] and pre-rRNAs [7]. In contrast to the majority of other NBs, a large number (several hundred per nucleus) of iPNBs is induced simultaneously, and they are uniformly distributed within the nuclear space [7].

The analysis of NB mobility is a complex problem as living cells move and deform during image acquisition. The observed motions consist of two components: a local motion of the NBs and a global motion of the nucleus (displacement and deformation) that should be compensated prior to the NB mobility analysis. The global motion of the nucleus can be ignored if the nucleus is relatively immobile and the time of observation is short, but correct description of intranuclear motility is impossible without compensation for global mobility of the nucleus before particle tracking and trajectory analysis. Here, we describe the pipeline for the NB mobility analysis that allows plotting the trajectories of the NBs within the nucleus taking into account the global movement of the nucleus (Fig. 1). We describe a 2D contour-based image registration protocol for compensation of the motion and deformation of the nucleus in fluorescence microscopy time-lapse sequences [9]. Our pipeline also allows to

classify the observed NB motion into simple diffusion (Brownian diffusion), constrained diffusion or directed (flow) diffusion [10]. It should be stressed that the described approach may be adapted for the mobility analysis of other NBs or discrete nuclear compartments.

2 Materials

2.1 Cells

HeLa cell line was originally obtained from the Russian Cell Culture Collection (Institute of Cytology of the Russian Academy of Sciences, Saint Petersburg, Russia) (*see* **Note 1**).

2.2 Cell culture

1. Dulbecco's modified Eagle's medium (DMEM) (Paneco).
2. Alanine-glutamine (Paneco).
3. Fetal calf serum (HyClone).
4. Antibiotic-antimycotic mixture (Gibco).
5. Hank's balanced salt solution (Paneco).
6. GFP-NPM WT plasmid (Addgene plasmid no. 17578, a gift from Dr. X.W. Wang [11]).
7. Lipofectamine 2000 (Invitrogen).

2.3 Cell culture plastic

1. Ventilated T125 flasks (Eppendorf).
2. 35-mm dishes with a coverslip (MatTek).
3. 15 mL centrifuge tubes (Greiner).

2.4 Microscopy

1. Nikon C2 scanning confocal microscope mounted on a motorized inverted microscope Eclipse Ti-E (Nikon) (*see* **Note 2**).
2. Innova CO-170 CO_2 incubator (New Brunswick Scientific).

2.5 Image analysis software

1. NIS-Elements Microscope Imaging Software (Nikon) (*see* **Note 2**).

2. FIJI (https://fiji.sc/).

3. ICY (http://icy.bioimageanalysis.org/).

4. Matlab (MathWorks) with DIPimage toolbox (http://www.diplib.org).

5. Excel (Microsoft).

6. NB tracking pipeline (https://gitlab.com/dsorokin.msk/mmb-ipnb-tracking).

3 Methods

3.1 Cell culture

HeLa cells were maintained in DMEM supplemented with alanine-glutamine, 10% fetal calf serum and an antibiotic and antimycotic mixture. Approximately 10^5 cells were seeded onto 35 mm Petri dishes with the glass bottom. Cells were then transfected with the GFP-NPM WT plasmid using the Lipofectamine 2000 reagent according to the manufacturer's instructions (*see* **Note 3**).

3.2 Induction of iPNB formation (*see* Note 4)

All operations should be carried out at 37°C unless indicated otherwise.

1. Prepare the hypotonic solution (20% Hank's solution) (*see* **Note 5**). Use at least 5 ml of hypotonic solution pre-warmed to 37°C per one 35 mm Petri dish.

2. Remove growth medium from the Petri dish and briefly wash cells with ~2 ml of the hypotonic solution.

3. Incubate cells in a second change of the hypotonic solution (~2 ml) for 15 min at 37°C in the CO_2-incubator.

4. Wash cells with the complete growth medium, and then incubate cells in the complete growth medium for ~20 min at 37°C in the CO_2-incubator (*see* **Note 6**).

3.3 Live-cell imaging

1. Use an inverted confocal microscope suitable for live experiments, i.e., equipped with a humidified thermostatic chamber with the CO_2 level maintenance.

2. Use a high aperture objective, e.g. Nikon Plan Apo VC 60/1.40 Oil or equivalent.

3. Identify transfected cell and focus in the center of the nucleus.

4. Capture a time lapse movie. Use the following parameters as a starting point and adjust them if needed: scale factor - 0.05 μm/pixel, FPS - 2 frame/sec, duration - 2 min.

5. Use the FIJI software or the provided microscope software to export the captured movie into the multipage TIFF format.

3.4 Image analysis

The input image sequences should be in the multipage TIFF format. All further operations are performed in Matlab except for the iPNB tracking which is performed using freely available ICY software with the Spot Tracking plugin [12]. The Matlab code including precompiled libraries can be downloaded at https://gitlab.com/dsorokin.msk/mmb-ipnb-tracking. The detailed description of the pipeline and the adjustable parameters can be found in the *main_script.m* file. The pipeline is shown in Fig.1 and is described in more detail below:

1. Image sequence preprocessing (*preprocessSequence.m*). At this stage, we equilibrate image intensities of every frame. As a result, the image intensities of all frames should be within the same range.

2. Nucleus segmentation (*nucleusSegmentation.m*). Here we segment the nucleus (identify the contours) using a threshold-based approach. The threshold type and other parameters can be adjusted depending on the data.

3. Nuclear body detection (*findNuclearBodies.m*). At this stage we segment the nuclear bodies using a combination of threshold-based approach for larger bodies (e.g., nucleoli) and blob detection-based approach [13] for smaller bodies (e.g., iPNBs) (Fig. 2).

4. Nuclear body tracking using the ICY Spot Tracking plugin:

- Importing the results of the previous step ("**_spots_ICY.txt*") into the ICY software using Plugins → Spot Detection Import and Export → Import.

- Tracking using the Spot Tracking plugin: choose spots imported in the previous step as Detection set, Estimate parameters, Run tracking.

- Export the tracking results from Track Manager to "**_tracks.xml*" using File → Save As…

5. Conversion of tracks to Matlab format and postprocessing of the tracks by joining adjacent subtracks (*convertTracksToMatlab.m*).

6. Nucleus motion compensation and application of the obtained deformation fields to track coordinates (*compensateGlobalMotion.m*). At this stage the nucleus motion is estimated using the non-rigid elasticity-based approach. The obtained motion is applied to the NB tracks to compensate the motion of the nucleus (*see* Fig. 3 for comparison between the original and compensated NB tracks).

7. Computation of track statistics and determination of the motion type and pattern for each NB (*analyzeTracksMotionType.m*) (*see* **Note 7** and Fig. 4).

4 Notes

1. Different adherent cultured cells may be used for the analysis if NB mobility. Suspension cells can be immobilized on polylysine-coated slides or grown in soft agar.

2. Other microscopy systems may be used for image recording. The input image sequences should be in the multipage TIFF format.

3. The described approach can be applied to different NBs. If the work is carried out with other NBs, then a plasmid coding for the most abundant proteins of these NBs should be used.

4. This step is necessary only for iPNBs. It should be omitted when studying other NBs.

5. iPNBs formation may start during hypotonic treatment if 20% Hanks solution is used (unpublished data). It appears that HeLa cells can adapt to hypotonic conditions, which leads to iPNB formation before the return to isotonic conditions. We believe that this cannot substantially influence NB dynamics, but, nevertheless, it is possible to use 10% Hank's solution (10 min) instead of 20% solution. In this case, more robust hypotonic conditions do not allow cells to adapt.

6. The optimal time for the start of iPNB imaging is 25-35 min after the return to isotonic conditions. At this stage, the number of iPNBs is substantially reduced [7], facilitating the imaging and analysis of iPNBs tracks. Cells can be incubated directly on the microscope stage, if the thermostatic chamber allows to control both CO_2 and temperature. In this case, it is necessary to work in the darkroom (at least to turn off the light immediately after mounting of the Petri dish inside the thermostatic chamber). The mobility of other NBs may be registered immediately after mounting of the Petri dish on the microscope stage. The optimal duration of live-cell imaging will depend on specific experimental conditions and the type of NB studied. It is also possible to acquire several cells in one experiment.

7. The mean square displacement (MSD) curve analysis approach described in [10] is used for classification of NB motion patterns. Briefly, the motion can be classified into three types: simple diffusion (Brownian diffusion), constrained diffusion and directed diffusion (flow). To determine the type of motion represented by the trajectory, we found the best fit for the calculated MSD using the analytical expressions for the different diffusion models [14] with localization uncertainty described in [15]. Fitting of analytical curves to experimental data obtained from track analysis can be performed using the Nelder-Mead optimization method [16]. The analysis pipeline outputs the first frame of microscopy image sequence with the tracks depicted on it with enclosing ellipses of different colors corresponding to the iPNB motion types (black, constrained diffusion, green, simple diffusion, cyan, directed diffusion).

It also outputs the statistics of the tracks including track length, iPNB initial position (px), track enclosing ellipse area (micron^2), total traveled distance (micron), average distance per frame (micron), standard deviation of distance per frame (μm), average velocity (μm/s), diffusion coefficient (μm$^{2/s}$ * 10^{-5}), particle diffusion velocity (μm/s * 10^{-3}) or confinement area (μm^2 * 10^{-3}) depending on the type of motion. An example of the output statistics in an Excel file is shown in Fig. 4.

Acknowledgements

We are grateful to Dr. X.W. Wang for the GFP-NPM WT plasmid. The work was supported by the Russian Science Foundation (17-11-01279 to DVS for image analysis) and the Russian Foundation for Basic Research (project 18-54-16002 to EVS for cell preparation and microscopy).

References

1. Dundr M (2012) Nuclear bodies: multifunctional companions of the genome. Curr Opin Cell Biol 24:415–422. https://doi:10.1016/j.ceb.2012.03.010
2. Iarovaia OV, Minina EP, Sheval EV, Onichtchouk D, Dokudovskaya S, Razin SV, Vassetzky YS (2019) Nucleolus: a central hub for nuclear functions. Trends Cell Biol https://doi:10.1016/j.tcb.2019.04.003
3. Arifulin EA, Musinova YR, Vassetzky YS, Sheval EV (2018) Mobility of nuclear components and genome functioning. Biochemistry (Moscow) 83(3):690–700. https://doi:10.1134/S0006297918060068
4. Zatsepina OV, Dudnic OA, Todorov IT, Thiry M, Spring H, Trendelenburg MF (1997) Experimental induction of prenucleolar bodies (PNBs) in interphase cells: interphase PNBs show similar characteristics as those typically observed at telophase of mitosis in

untreated cells. Chromosoma 105:418–430.

5. Musinova YR, Lisitsyna OM, Golyshev SA, Tuzhikov AI, Polyakov VY, Sheval EV (2011) Nucleolar localization/retention signal is responsible for transient accumulation of histone H2B in the nucleolus through electrostatic interactions. Biochim Biophys Acta 1813:27–38. https://doi:10.1016/j.bbamcr.2010.11.003
6. Musinova YR, Kananykhina EY, Potashnikova DM, Lisitsyna OM, Sheval EV (2015) A charge-dependent mechanism is responsible for the dynamic accumulation of proteins inside nucleoli. Biochim Biophys Acta 1853:101–110. https://doi:10.1016/j.bbamcr.2014.10.007
7. Musinova YR, Lisitsyna OM, Sorokin DV, Arifulin EA, Smirnova TA, Zinovkin RA, Potashnikova DM, Vassetzky YS, Sheval EV (2016) RNA-dependent disassembly of nuclear bodies. J Cell Sci 129:4509–4520. https://doi:10.1242/jcs.189142
8. Pellar GJ, DiMario PJ (2003) Deletion and site-specific mutagenesis of nucleolin's carboxy GAR domain. Chromosoma 111:461–469. https://doi:10.1007/s00412-003-0231-y
9. Sorokin DV, Peterlik I, Tektonidis M, Rohr K, Matula P (2018) Non-rigid contour-based registration of cell nuclei in 2-D live cell microscopy images using a dynamic elasticity model. IEEE Trans Med Imaging 37(1):173-184. https://doi:10.1109/TMI.2017.2734169
10. Arifulin EA, Sorokin DV, Tvorogova AV, Kurnaeva MA, Musinova YR, Zhironkina OA, Golyshev SA, Abramchuk SS, Vassetzky YS, Sheval EV (2018) Heterochromatin restricts the mobility of nuclear bodies. Chromosoma 127:529–537. https://doi:10.1007/s00412-018-0683-8
11. Wang W, Budhu A, Forgues M, Wang XW (2005) Temporal and spatial control of nucleophosmin by the Ran-Crm1 complex in centrosome duplication. Nat Cell Biol 7:823–830. https://doi:10.1038/ncb1282

12. Chenouard N, Bloch I, Olivo-Marin J-C (2013) Multiple hypothesis tracking for cluttered biological image sequences. IEEE Trans Pattern Anal Mach Intell 35:2736–3750. https://doi:10.1109/TPAMI.2013.97

13. Foltánková V, Matula P, Sorokin D, Kozubek S, Bártová E (2013) Hybrid detectors improved time-lapse confocal microscopy of PML and 53BP1 nuclear body colocalization in DNA lesions. Microsc Microanal 19(2),360–369. http://doi:10.1017/S1431927612014353

14. Daumas F, Destainville N, Millot C, Lopez A, Dean D, Salomé L (2003) Confined diffusion without fences of a g-protein-coupled receptor as revealed by single particle tracking. Biophys J 84:356–366. https://doi:10.1016/S0006-3495(03)74856-5

15. Michalet X (2010) Mean square displacement analysis of single-particle trajectories with localization error: Brownian motion in an isotropic medium. Phys Rev E Stat Nonlin Soft Matter Phys 82:041914. https://doi:10.1103/PhysRevE.82.041914

16. Nelder JA, Mead R (1965) A simplex method for function minimization. The computer journal 7(4):308–313. https://doi.org/10.1093/comjnl/7.4.308

Figure legends:

Fig. 1 The pipeline for the NB mobility analysis.

Fig. 2 Representative images of the nucleus segmentation (**A**), nucleolus detection by a threshold-based approach (**B**), iPNB detection by a blob detection-based approach (**C**), resulting NB detection (**D**). Scale bar = 5 μm.

Fig. 3 Example of non-rigid compensation for global nucleus motion. The analysis pipeline outputs the first frame of microscopy image sequence with the tracks depicted on it with enclosing ellipses of different colors corresponding to the iPNB motion types (black, constrained diffusion, green, simple diffusion). **A**, iPNB tracks plotted over the first frame of the image sequence without compensation for nucleus non-rigid motion; **B**, the compensating deformation field plotted over the image (the length of the vectors and spacing between them were enlarged for better visibility); **C**, iPNB tracks after compensation for the nucleus motion; **D** and **E** are the enlarged fragments of **A** (non-compensated motion) and **C** (compensated motion), respectively. The dominant direction of iPNBs motion, which is a result of global nucleus motion, is indicated by an arrow in (**D**). Scale bar =5 μm in A-C and 1 μm in D and E.

Fig. 4 Example of track visualization and output statistics in an Excel file as a result of the NB tracking pipeline (https://gitlab.com/dsorokin.msk/mmb-ipnb-tracking).

Image sequence preprocessing

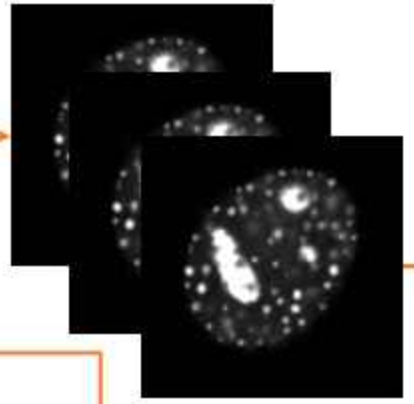

Nuclear bodies detection

Nuclear bodies tracking

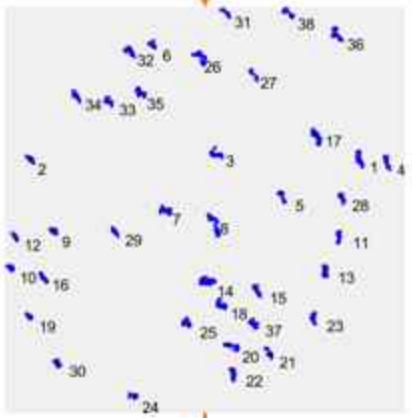

Nucleus segmentation

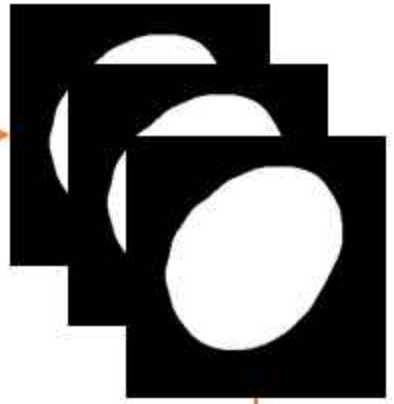

Nucleus motion estimation

Nucleus motion compensation

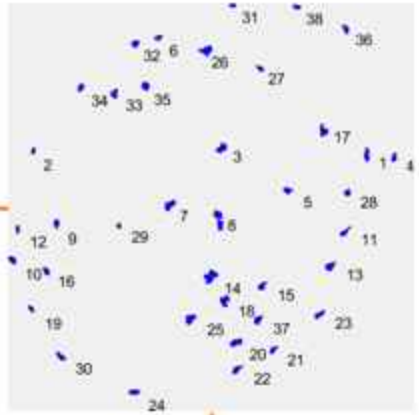

Computation of tracks statistics

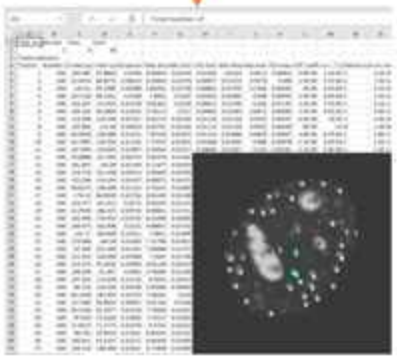

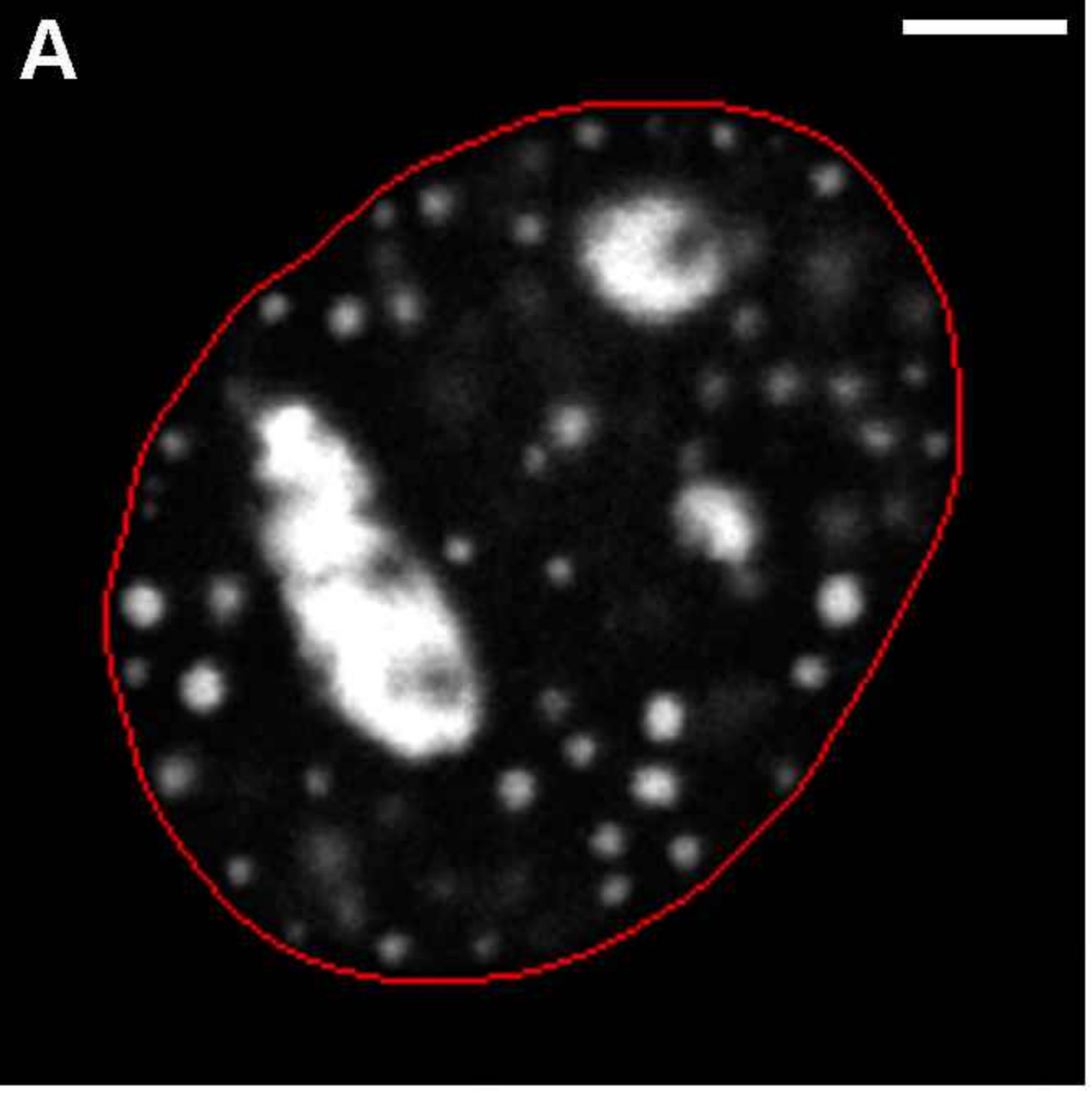
A

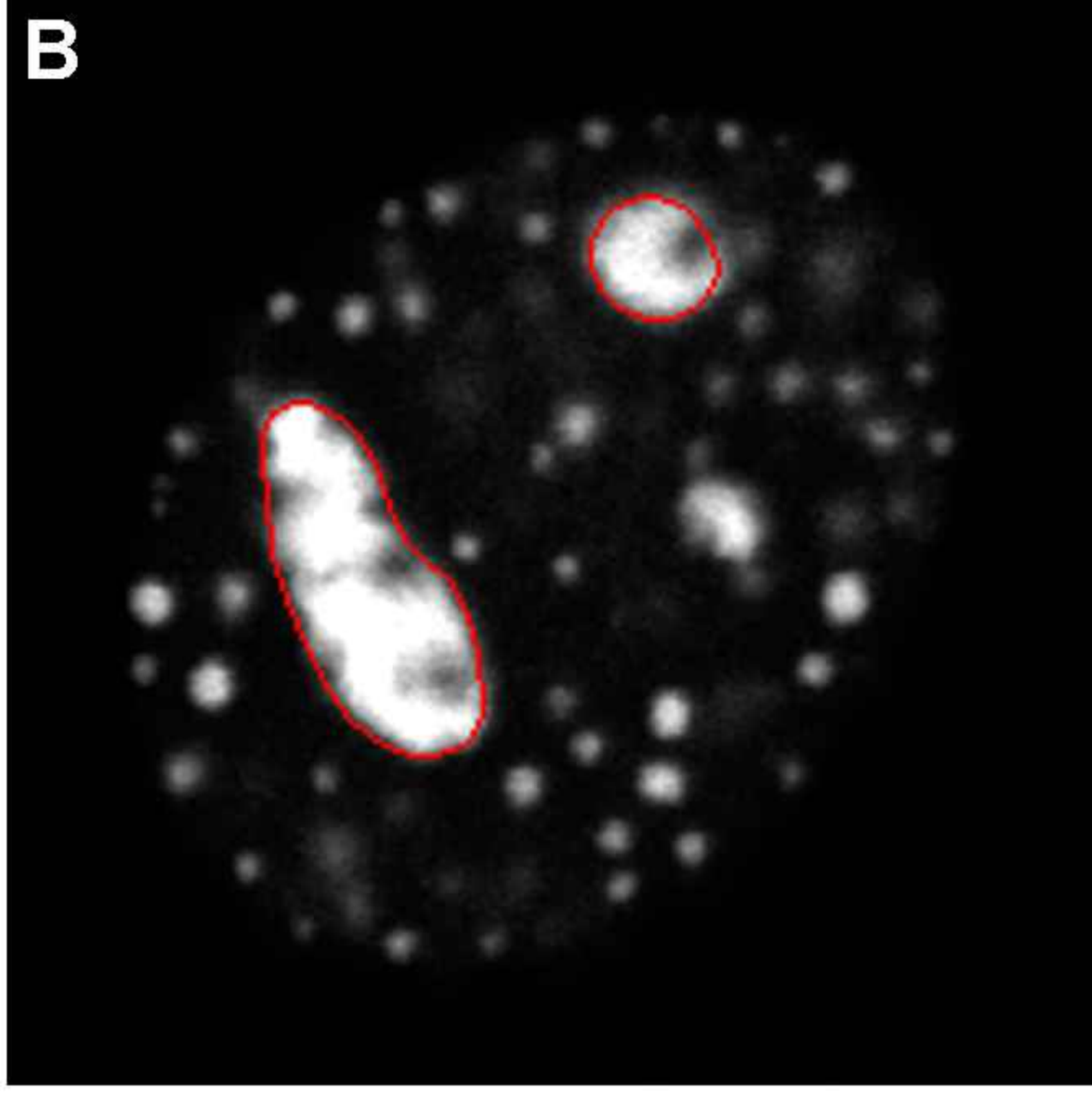
B

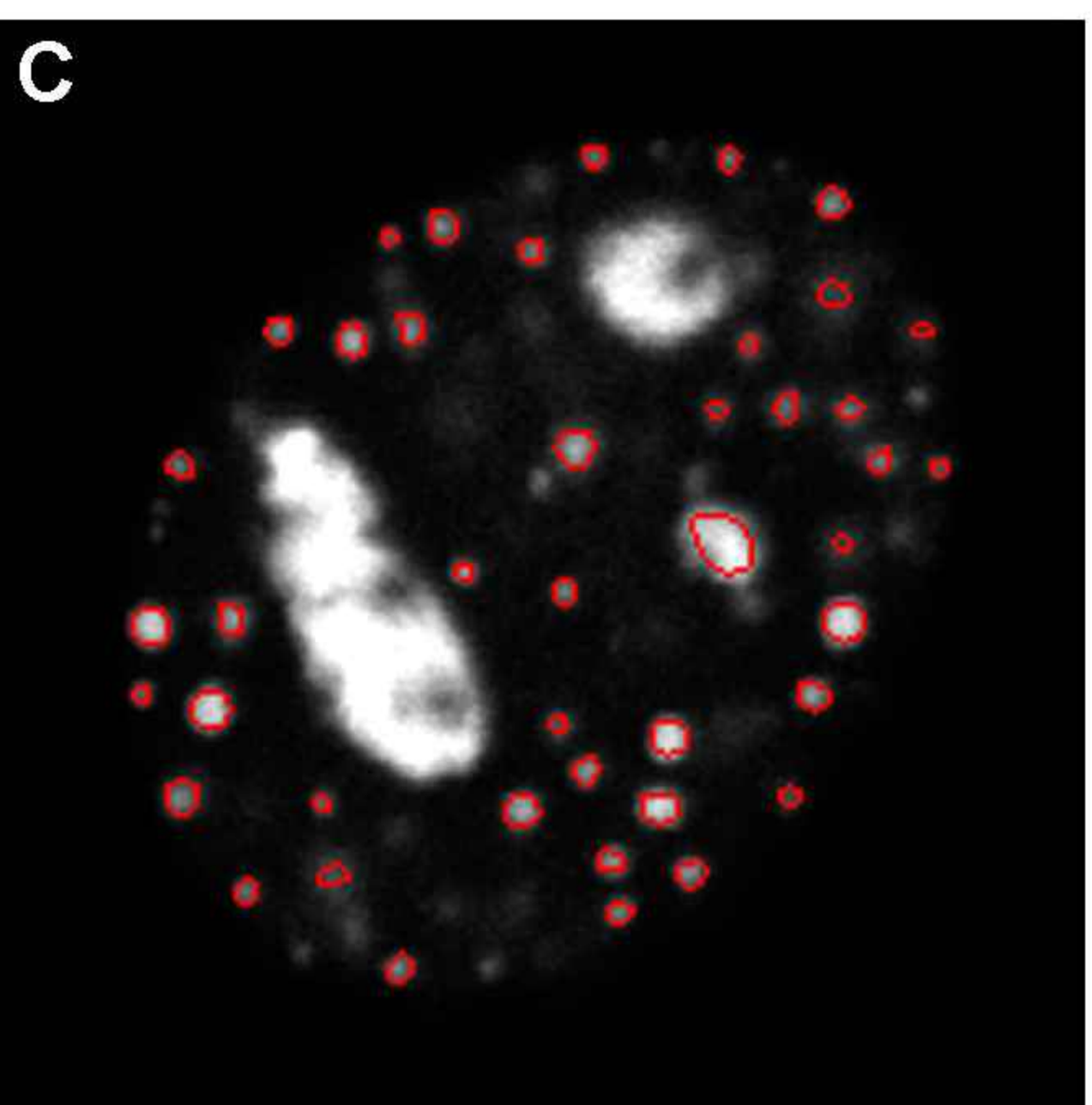
C

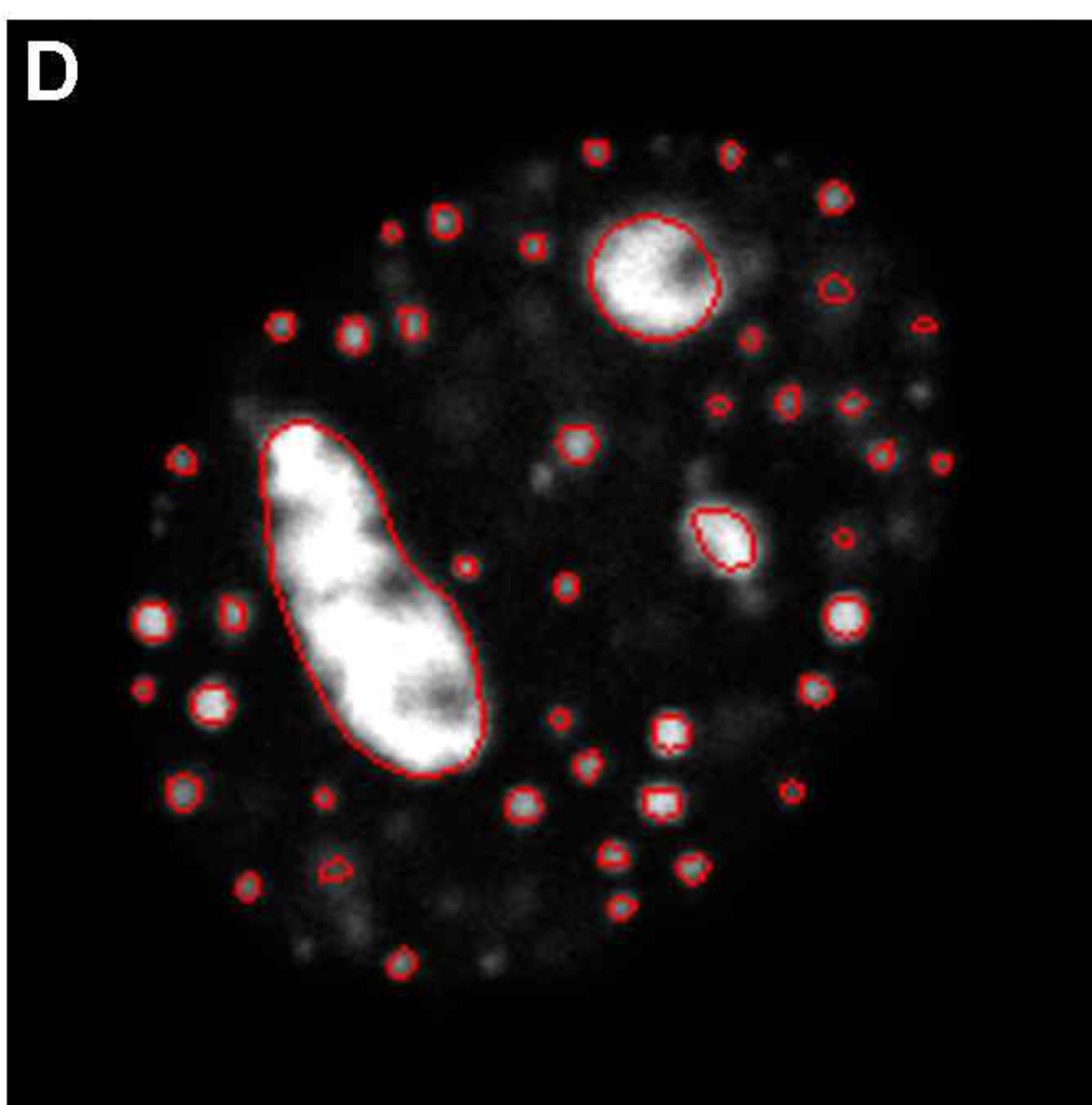
D

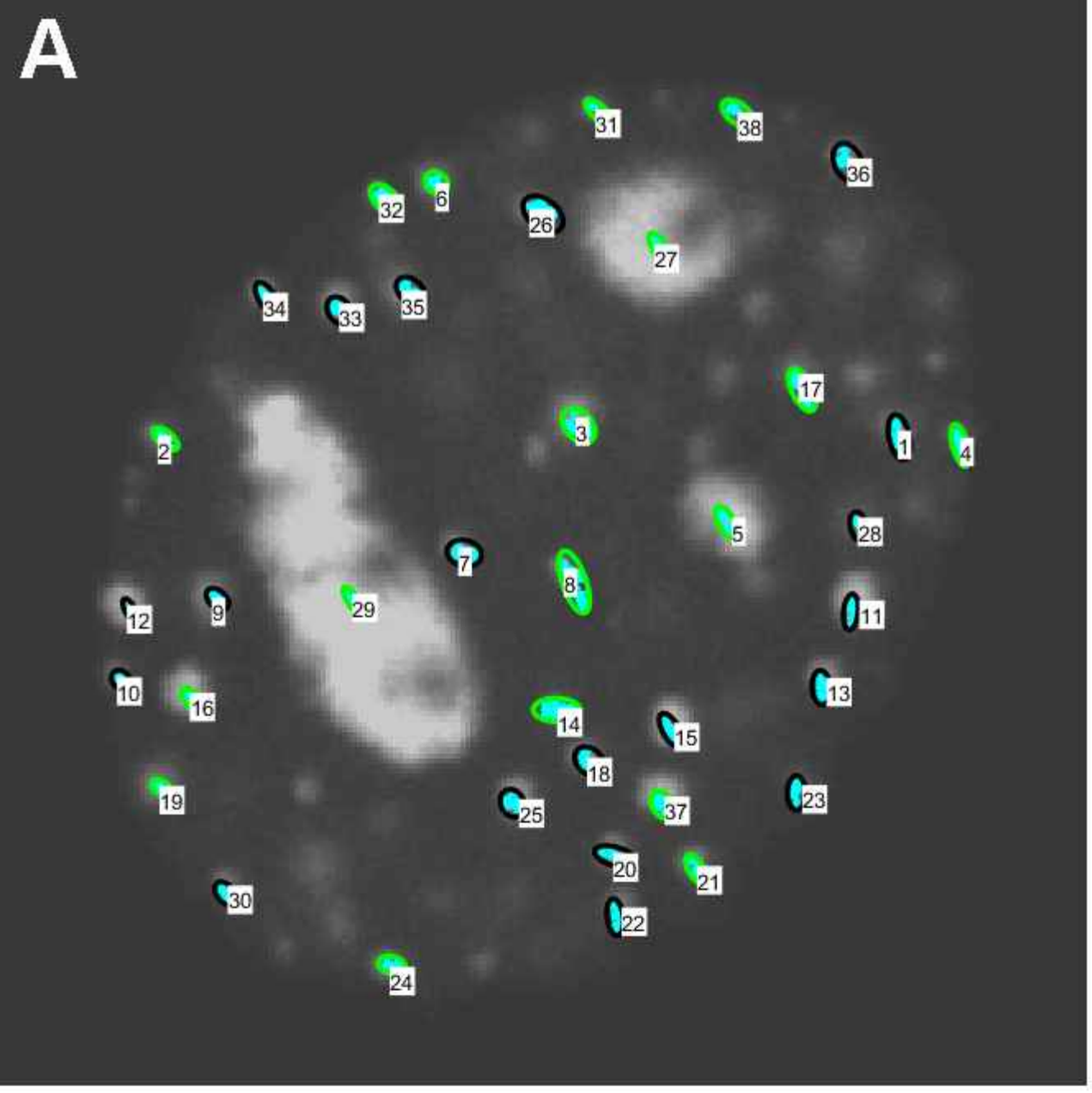
A
31
38
36
32
6
26
27
34
33
35
17
3
2
1
4
5
28
7
8
29
12
9
11
10
16
13
14
15
18
19
25
37
23
20
21
30
22
24

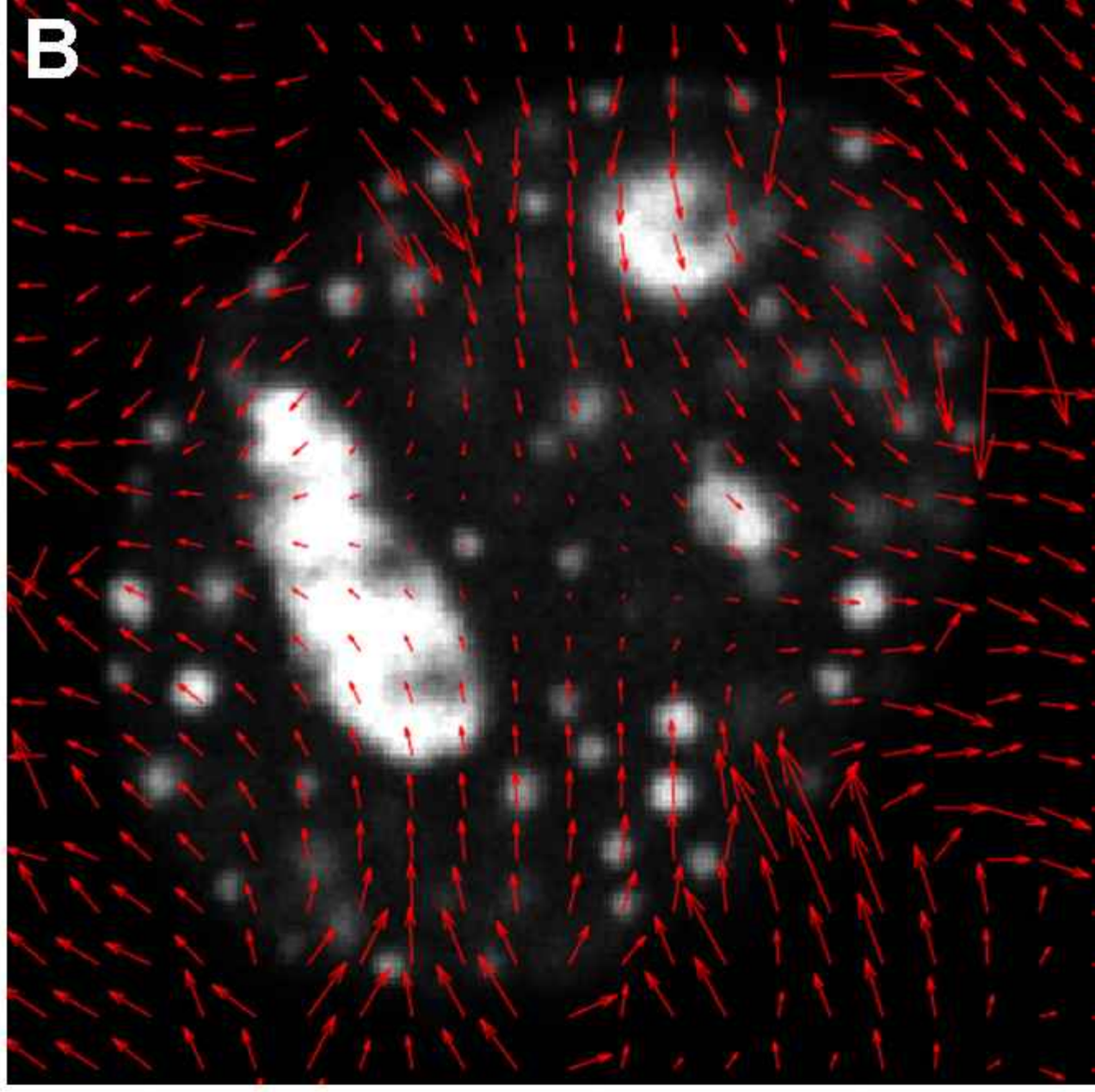
B

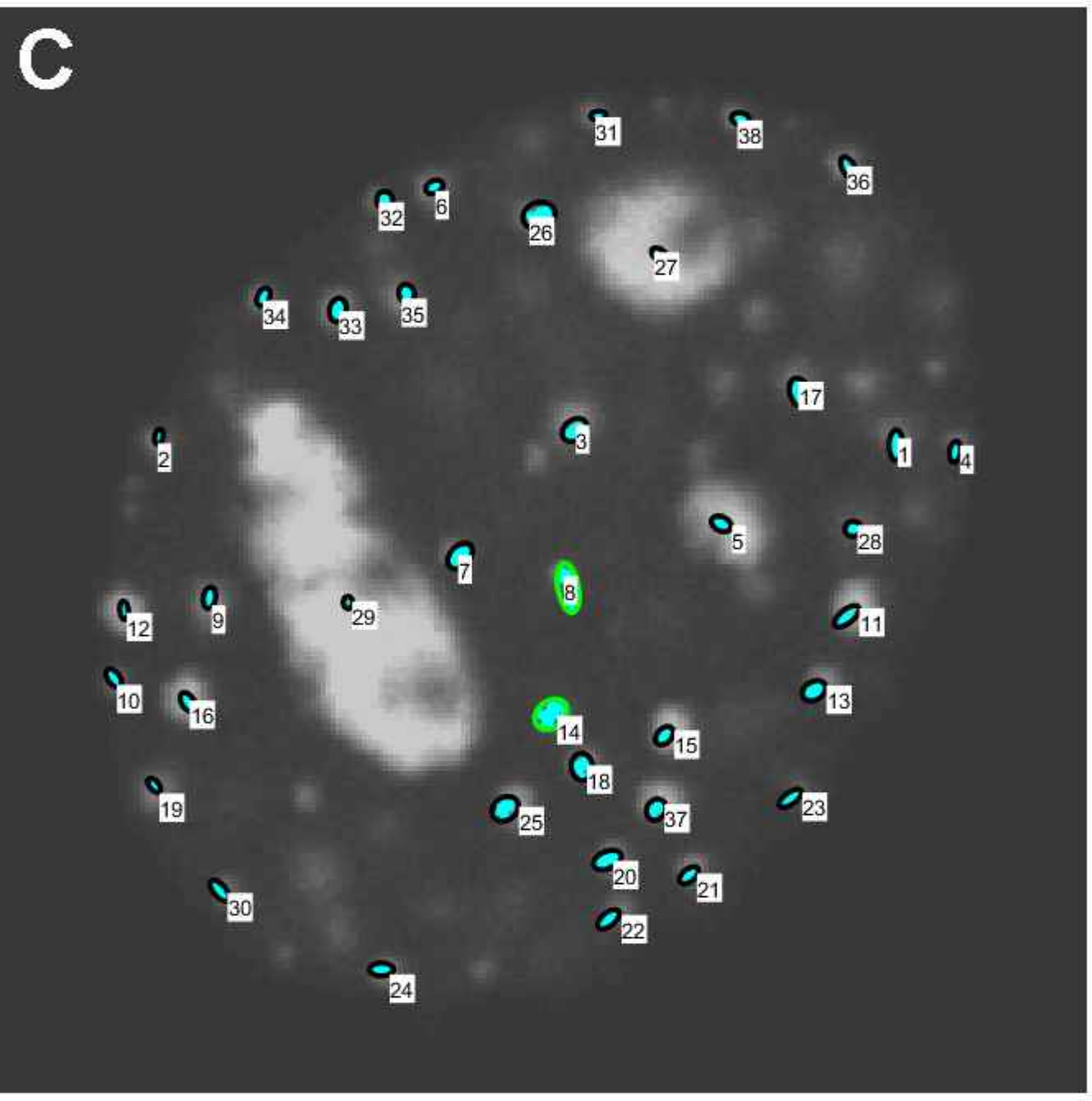
C
31
38
36
32
6
26
27
34
33
35
17
3
2
1
4
5
28
7
8
29
12
9
11
10
16
13
14
15
18
19
25
37
23
20
21
30
22
24

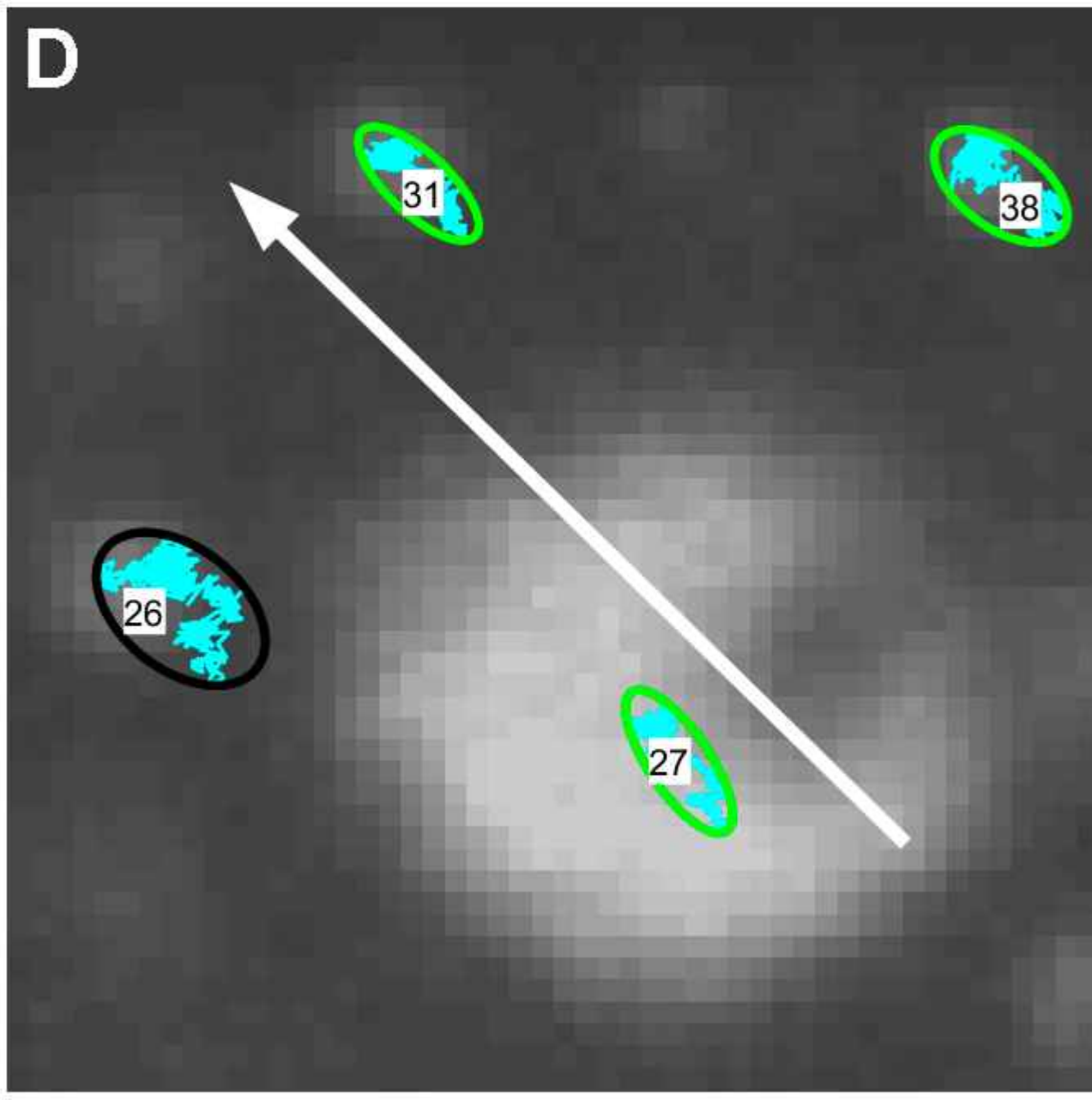
D
31
38
26
27

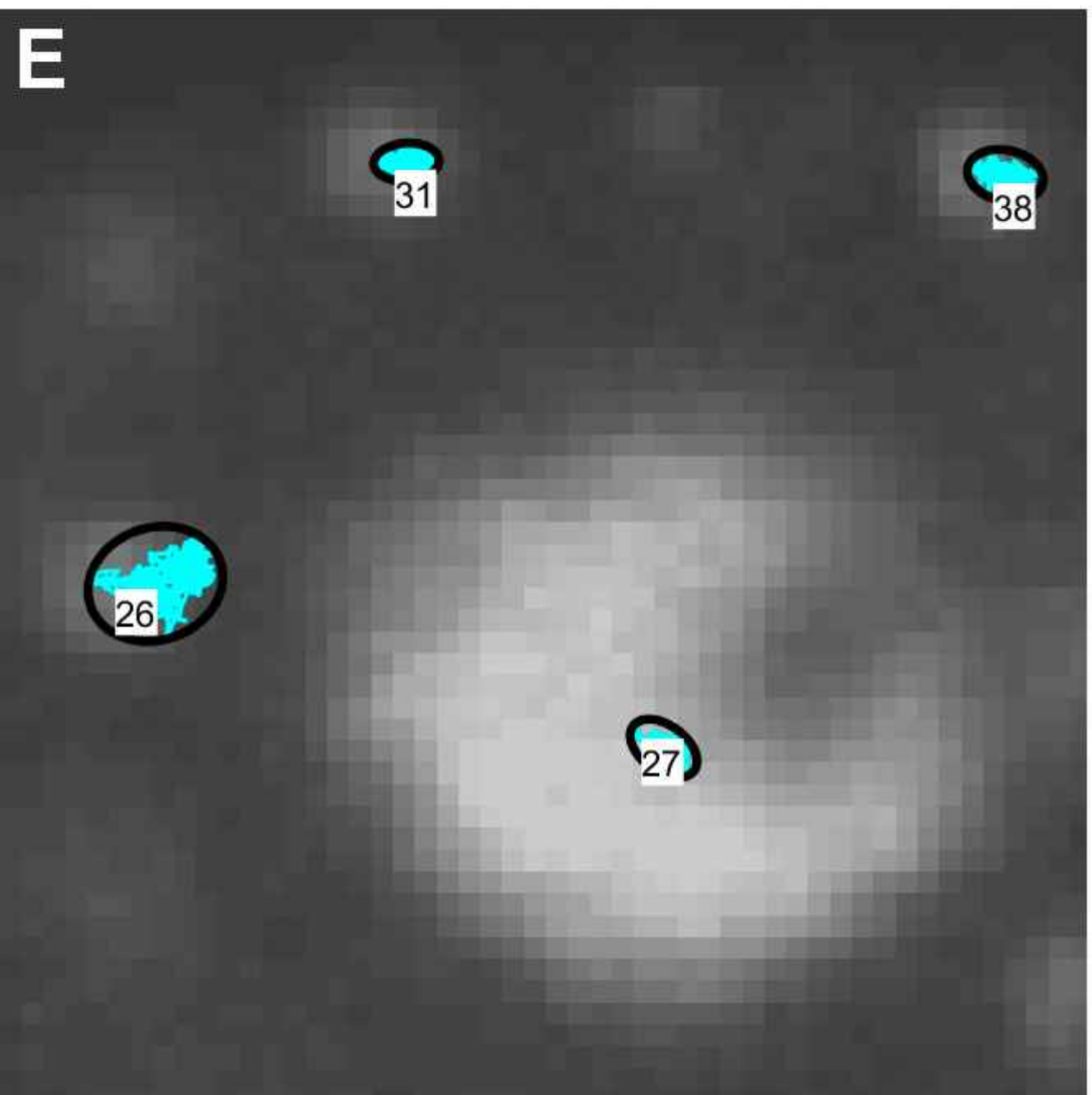
E
31
38
26
27

	A	B	C	D	E	F	G	H	I	J	K	L	M	N	O
1	Total numb	Normal	Flow	Conf											
2		2	0	36											
3	Tracks statistics:														
4	TrackID	Number Of	X start (px)	Y start (px)	Ellipse Area	Total dist. (	AVG Dist-p	STD Dist-p	AVG Veloc	AVG area (r	STD area (n	Diff. coeff.	v or L * 10^	Motion type	Error norm
5	1	400	195,3834	97,88288	0,019598	8,959345	0,022454	0,013038	0,022398	0,0512	0,008126	6,91E-09	1,13E-05	C	3,24E-10
6	2	400	52,64243	98,82746	0,006139	6,298344	0,015785	0,009371	0,015746	0,0576	0,005997	2,39E-09	5,66E-06	C	7,34E-12
7	3	400	133,3104	95,29854	0,025885	6,820622	0,017094	0,008908	0,017052	0,1056	0,004554	3,96E-09	6,24E-06	C	3,2E-10
8	4	400	207,4278	99,22006	0,010796	7,859096	0,019697	0,010623	0,019648	0,048	0,005415	2,5E-09	8,41E-06	C	1,26E-12
9	5	400	163,4668	114,6327	0,013781	5,823617	0,014596	0,00812	0,014559	0,264	0,011548	3,18E-09	4,68E-06	C	6,13E-11
10	6	400	106,181	50,09653	0,010521	6,781144	0,016995	0,009946	0,016953	0,0672	0,005848	2,4E-09	6,51E-06	C	5,61E-12
11	7	400	110,5988	120,4475	0,027614	8,63713	0,021647	0,011359	0,021593	0,0432	0,003468	6,26E-09	1E-05	C	3,48E-10
12	8	400	130,9818	124,4902	0,048155	8,637007	0,021647	0,01113	0,021593	0,0592	0,004394	8E-09	1,6	N	1,41E-09
13	9	400	63,06494	130,0888	0,012408	7,873186	0,019732	0							
14	10	400	44,76647	145,4341	0,011561	7,743746	0,019408	0							
15	11	400	187,9928	130,6556	0,018966	6,26934	0,015713	0							
16	12	400	46,68883	131,5653	0,007445	5,954788	0,014924	0							
17	13	400	181,6667	145,5801	0,021687	8,11677	0,020343	0							
18	14	400	129,7188	151,458	0,044139	9,595627	0,024049	0							
19	15	400	152,2964	154,2643	0,014374	6,683717	0,016751	0							
20	16	400	58,81734	148,4984	0,012245	6,754414	0,016928	0							
21	17	400	176,2204	86,90581	0,027562	8,651954	0,021684	0							
22	18	400	135,477	161,0121	0,027199	8,502639	0,02131	0							
23	19	400	52,97048	166,4254	0,007433	6,908306	0,017314	0							
24	20	400	140,4978	179,4535	0,023763	8,310954	0,020829	0							
25	21	400	156,6735	181,9078	0,013105	6,988724	0,017516	0							
26	22	400	142,1702	189,9094	0,016107	7,963098	0,019958	0							
27	23	400	176,9683	166,2799	0,014625	7,227894	0,018115	0							
28	24	400	97,39301	201,3686	0,014424	7,008978	0,017566	0							
29	25	400	122,3246	169,0078	0,029975	7,046701	0,017661								
30	26	400	124,314	55,06349	0,040586	9,631284	0,024139	0							
31	27	400	148,3952	61,93705	0,009199	4,784838	0,011992	0							
32	28	400	187,6533	114,6381	0,011261	8,035101	0,020138								
33	29	400	90,19204	129,3359	0,005482	3,959661	0,009924	0							
34	30	400	66,10481	185,6555	0,014792	7,58281	0,019005	0							
35	31	400	137,0833	35,8645	0,006507	6,621448	0,016595	0							
36	32	400	95,31061	52,26768	0,013281	7,70636	0,019314	0							
37	33	400	87,63397	73,3294	0,018932	7,755171	0,019437	0							
38	34	400	72,93154	71,2773	0,010791	6,4762	0,016231	0							
39	35	400	99,70296	70,85252	0,01401	8,901622	0,02231	0							
40	36	400	185,6414	45,31066	0,013706	6,644051	0,016652	0							
41	37	400	150,4146	168,499	0,019212	6,71838	0,016838	0							
42	38	400	164,4793	36,46553	0,010244	7,323825	0,018355	0